BIODIVERSITAS
Volume 26, Number 10, October 2025
Pages: 5156-5168

ISSN: 1412-033X
E-ISSN: 2085-4722
DOI: 10.13057/biodiv/d261030

Phytochemical screening, antimicrobial and antidiabetic activity of *n*-hexane extract of *Macaranga depressa* leaves

KHOLIFATU ROSYIDAH[1,♥], RAHMAT EKO SANJAYA[1], UTAMI IRAWATI[1], NAWWAL HIKMAH[1], RIZKY AULIA FITRIANI[1], JANNESA TRI ROSADI[1], IRAWAN WIJAYA KUSUMA[2], YADI[3], AGNES V. SIMAMORA[4], ANTONIUS R. B. OLA[5], I GUSTI MADE NGURAH BUDIANA[6]

[1]Department of Chemistry, Faculty of Mathematics and Natural Sciences, Universitas Lambung Mangkurat. Jl. A. Yani Km. 36, Banjarbaru 70714, South Kalimantan, Indonesia. Tel./fax.: +62-511-4773112, ♥email: krosyidah@ulm.ac.id
[2]Faculty of Forestry and Tropical Environment, Universitas Mulawarman. Jl. Penajam, Samarinda 75119, East Kalimantan, Indonesia
[3]Faculty of Medicine, Universitas Mulawarman. Jl. Kerayan, Samarinda 75119, East Kalimantan, Indonesia
[4]Department of Agrotechnology, Faculty of Agriculture, Universitas Nusa Cendana. Jl. Adisucipto, Kupang 85001, East Nusa Tenggara, Indonesia
[5]Department of Chemistry, Faculty of Science and Engineering, Universitas Nusa Cendana. Jl. Adisucipto, Kupang 85001, East Nusa Tenggara, Indonesia
[6]Department of Chemistry Education, Faculty of Teacher Training and Education, Universitas Nusa Cendana. Jl. Adisucipto, Kupang 85001, East Nusa Tenggara, Indonesia

Manuscript received: 1 July 2025. Revision accepted: 14 October 2025.

Abstract. *Rosyidah K, Sanjaya RE, Irawati U, Hikmah N, Fitriani RA, Rosadi JT, Kusuma IW, Yadi, Simamora AV, Ola ARB, Budiana IGMN. 2025. Phytochemical screening, antimicrobial and antidiabetic activity of n-*hexane *extract of* Macaranga depressa *leaves. Biodiversitas 26: 5156-5168.* The *Macaranga* genus has been used in folk medicine to treat pathological disorders like diabetes. However, the chemical constituents and bioactivity of *Macaranga depressa* have never been studied. Thus, this study combined phytochemical profiling, antimicrobial evaluation, and in silico molecular docking of *M. depressa*. It aims to determine the phytochemical profile, antimicrobial, and antidiabetic activities of *n*-hexane extract of *M. depressa* leaves. Sample extraction was carried out by maceration method. The phytochemical profile of the plant was determined by phytochemical screening method and analyzed using Gas Chromatography-Mass Spectrometry (GC-MS) method. Antimicrobial activity was tested in vitro using disc diffusion method. Antidiabetic activity was tested in vitro and in silico including drug similarity analysis, ADME (Absorption, Distribution, Metabolism, and Excretion) pharmacokinetic profile, toxicity potential, and molecular docking interaction. Phytochemical screening revealed the presence of alkaloids, flavonoids, terpenoids, and tannins. GC-MS analysis identified stigmast-4-e*n*-3-one (32.76%) and 4',6'-dimethoxy-2'-hydroxy-3-nitrochalcone (14.82%) as the major components. The extract exhibited significant antimicrobial activity against *Candida albicans* (18.0±0.44 mm), *Escherichia coli* (19.4±0.57 mm), *Pseudomonas aeruginosa* (23.5±1.32 mm), and *Staphylococcus aureus* (21.2±0.47 mm). The in vitro antidiabetic test using the α-glucosidase enzyme showed that the *n*-hexane extract of *M. depressa* had an IC_{50} value of 17.561±0.471 ppm. ADMET analysis indicated that the major components followed Lipinski's rule, exhibited drug-like properties, and were no*n*-mutagenic. Molecular docking results showed strong interactions between the major compounds and maltase-glucoamylase (2QMJ) and PPAR-γ (2Q5S). These findings suggest that the *n*-hexane extract of *M. depressa* leaves has promising antimicrobial and antidiabetic potential.

Keywords: Antidiabetic, antimicrobial, *Macaranga depressa*, molecular-docking, phytochemical

INTRODUCTION

Infectious diseases caused by pathogenic bacteria and fungi continue to pose a significant global health challenge. In Indonesia alone, a 2017 public health survey reported approximately 2.5 million deaths annually attributable to infectious digestive diseases, with infections and parasitic conditions accounting for 35.1% of total mortality (Wijaya and Masfufatun 2022). Several pathogens commonly associated with severe infections include *Escherichia coli* as the leading cause of gastrointestinal and urinary tract infections (Zhou et al. 2023), *Staphylococcus aureus,* which causes skin infections (Sangboonruang et al. 2021), *Pseudomonas aeruginosa,* which causes wound infections and pneumonia (Wood et al. 2023), and *Candida albicans* as the cause of opportunistic fungal infections (Talapko et al. 2021). The challenge is further compounded by the rise of antimicrobial resistance, which diminishes the effectiveness of conventional antibiotics (Aldughaylibi et al. 2022).

Beyond the rising threat of infections, diabetes mellitus is emerging as a significant global health issue. Its prevalence is anticipated to rise from 2.8% in the year 2000 to approximately 4.4% by 2030. According to projections by the World Health Organization (WHO), diabetes may rank as the seventh leading cause of death worldwide by 2030 (Aldughaylibi et al. 2022). This metabolic disorder is marked by elevated blood glucose levels resulting from either insufficient insulin production or reduced insulin effectiveness. Diabetes is categorized into several types, including type 1, type 2, gestational diabetes, and other less common forms linked to genetic mutations or underlying conditions (Dilworth et al. 2021). When inadequately managed, the disease can lead to numerous complications, such as a heightened vulnerability to both bacterial and fungal infections (Rasoulpoor et al. 2021).

The rising incidence of infectious diseases and diabetes mellitus has encouraged the exploration of alternative therapeutic agents, particularly from medicinal plants known for their antimicrobial and antidiabetic potential. For centuries, herbal remedies have been utilized in traditional medicine due to their diverse bioactive constituents and pharmacological effects. Natural products have made significant contributions to the treatment of diabetes, with several modern drugs tracing their origins to plants and microbes. For example, metformin, the current first-line therapy for type 2 diabetes, can be linked back to the traditional use of *Galega officinalis* (goat's rue), where the plant alkaloid galegine inspired the development of the biguanides (Bailey 2017). Similarly, sodium-glucose cotransporter 2 (SGLT2) inhibitors, or gliflozins, were derived from phlorizin, a glycoside first isolated from apple tree bark in the 19th century (Fonseca-Correa and Correa-Rotter 2021). Another important drug, acarbose, used to control post-prandial glucose spikes, is a microbial natural product originally obtained from *Actinoplanes* species (Tsunoda et al. 2022).

The genus *Macaranga* has potential as a therapeutic agent. Traditionally, the leaves, bark, roots, flowers, and fruits of *Macaranga* plants are used for various folk remedies, including treating wounds, swelling, boils, fungal and bacterial infections, stomach aches, fever reducers, bruises, coughs, diabetes, anemia, laxatives, gastric ulcers, and hemorrhoids. Several *Macaranga* species have an important role in traditional medicine, including *Macaranga gigantea*, *M. triloba, M. hypoleuca*, *M. denticulata*, *M. hurifolia, M. barteri*, *M. peltata*, and *M. indica*. Several *Macaranga* members have demonstrated antioxidant, antimicrobial, anti-inflammatory, antidiabetic, and anticancer effects. Phytochemical studies of *Macaranga* species have reported the presence of various bioactive compounds, including prenylated, geranylated, and farnesylated flavonoids, stilbenes, terpenoids, tannins, coumarins, and steroids. Flavonoids and stilbenes are believed to be the main contributors to the pharmacological activity of this genus (Minarti et al. 2021; Kamso et al. 2022; Zeleke 2022; Rosamah et al. 2023; Preethi and Hedge 2025). However, specific studies on *Macaranga depressa* have not been reported either in terms of its phytochemical content or biological activities. This study aims to report the results of phytochemical screening of *n*-hexane extract of *M. depressa* leaves, compound content based on Gas Chromatography-Mass Spectrometry (GC-MS) analysis, antimicrobial tests against *Candida albicans, Escherichia coli, Pseudomonas aeruginosa,* and *Staphylococcus aureus* as well as antidiabetic tests in vitro through α-glucosidase inhibition and in silico using molecular docking.

MATERIALS AND METHODS

Preparation and isolation

Leaf samples of *Macaranga depressa* were collected from Sidomulyo Village, Kelumpang Hulu, Kotabaru, South Kalimantan, Indonesia (3°06'16.1" S 115°58'28.9" E) in April 2024. The species were identified at the Herbarium Wanariset, Samboja, and a voucher specimen had been deposited at Herbarium Wanariset, Samboja with document number: S.322/BPSILHK.SBJ/SBTU/SET.3.1/B/07/2024. The leaves were thoroughly washed with water to remove surface contaminants, then air-dried. Once completely dried, the samples were ground into fine powder using a laboratory blender and stored in airtight containers under dry conditions until extraction.

Extraction was performed using the maceration technique with *n*-hexane as the solvent. Powdered leaf material was soaked in *n*-hexane at a 1:5 (w/v) ratio in a glass container, stirred, and sealed with aluminum foil. The mixture was left to stand for 24 h before filtration to separate the liquid extract from the plant residue. This process was repeated twice (remaceration) using fresh solvent. The combined macerates were concentrated using a rotary evaporator at 50°C, followed by drying in a water bath at the same temperature to ensure complete solvent evaporation. The resulting residue constituted the dry *n*-hexane extract of *M. depressa* leaves.

Phytochemical screening

Phytochemical screening of the *n*-hexane extract of *M. depressa* leaves was conducted using standard qualitative procedures to detect the presence of alkaloids, flavonoids, terpenoids, tannins, and saponins.

Alkaloid detection

Two milliliters of the extract were placed in a test tube, followed by the addition of 2-3 drops of Mayer's reagent. A green precipitate indicated the presence of alkaloids. For further confirmation, the Wagner test was performed by adding a few drops of Wagner's reagent to another 2 mL portion of the extract. The formation of a reddish-brown precipitate supported the presence of alkaloids (Khanal 2021).

Flavonoid detection

Approximately 0.25 g of crude extract was combined with 10 mL of ethyl acetate and heated in a water bath for 3 minutes. After cooling, the mixture was filtered, and 4 mL of the filtrate was treated with 1 mL of dilute ammonia solution. A yellow coloration indicated a positive result for flavonoids (Gizaw et al. 2022).

Terpenoid detection

A portion of the extract was dissolved in 2 mL of chloroform and evaporated to dryness. Then, 2 mL of concentrated sulfuric acid was added. The appearance of a reddish-brown coloration on the surface indicated the presence of terpenoids (Khanal 2021).

Tannin detection

A 0.5 g sample of the extract was boiled with 10 mL of distilled water and filtered. Three drops of 0.10% ferric chloride solution were added to the filtrate. A brown, greenish, or blue-black color was taken as evidence of tannins (Gizaw et al. 2022).

Saponin detection

About 0.25 g of the extract was shaken with 5 mL of distilled water. The formation of persistent foam indicated the presence of saponins (Gizaw et al. 2022).

Antimicrobial test

The antimicrobial activity of the *n*-hexane extract from *M. depressa* leaves was assessed using the disk diffusion technique. A 0.3 mL suspension of bacteria (adjusted to 25% transmittance at 580 nm) and fungi (90% transmittance at 530 nm) was introduced into separate petri dishes. Nutrient agar (15 mL) was used for bacterial cultures, and potato dextrose agar (15 mL) for fungal cultures; both were poured into the dishes, mixed with the inoculum, and allowed to solidify. Sterile paper disks impregnated with 10 µL of the test extract were placed onto the surface of the solidified media. The plates were sealed and incubated at 37°C for 24 h for bacterial strains and at 25°C for 72 h for fungal strains. Antimicrobial activity was determined by measuring the diameter of the inhibition zones using a caliper (Hendriyani et al. 2024). The microbes used in the test are *Candida albicans*, *Escherichia coli*, *Pseudomonas aeruginosa*, and *Staphylococcus aureus.* Chloramphenicol was used as a positive control, and distilled water was used as a negative control. The concentration of both the sample and positive control was prepared at 2.5%.

GC-MS analysis

GC-MS analysis was carried out to identify the chemical content of *n*-hexane extract of *M. depressa* leaves. The analysis was performed using a GC-MS system (Agilent Technologies 7890A, USA) equipped with an autosampler (5975A), a mass-selective detector, and a ChemStation data processing system. A 5 µL aliquot of the filtered extract was injected into the instrument, with helium (He) as the carrier gas, delivered through a capillary column under constant pressure. The total flow rate was maintained at 1.2 mL/min, with a split ratio of 8:1. The injector and detector temperatures were set at 250°C and 230°C, respectively, while the oven temperature was programmed at 280°C and 140°C. The compounds were identified based on their mass spectral fragmentation patterns, which were compared against the National Institute of Standards and Technology (NIST-MS) database. The relative abundance of each compound was calculated based on the area percentage of its corresponding peak in the chromatogram (Masyudi et al. 2022).

Antidiabetic test

In vitro test

The α-glucosidase inhibitory assay was carried out as described by Etsassala et al. (2020). Phosphate buffer solution 0.1 M (pH 6.9) 50 µL, 10 µL of 1 ppm glucosidase enzyme, and 20 µL of sample or standard were added to the plate. Each concentration series was carried out in triplicate and incubated for 15 minutes at 37°C. After 10 minutes of incubation, 20 µL of 4-NPP (4-nitrophenyl β-d-glucopyranoside) was added to each well and incubated for 20 minutes at 37°C. The reaction was stopped by adding 50 µL of 0.1 M Na_2CO_3. The release of p-nitrophenol from the reaction mixture related to enzyme activity was read at a wavelength of 405 nm using a multiple reader (Multiskan, Thermo Scientific). Inhibition (%) was calculated based on equation below:

$$\%\text{Inhibition} = \frac{\text{Absorbance of blank} - \text{Absorbance of the sample}}{\text{Absorbance of blank}} \times 100\%$$

In silico assay

In silico evaluations of compounds present in the *n*-hexane extract of *M. depressa* were conducted, including analyses of drug-likeness, ADME (Absorption, Distribution, Metabolism, and Excretion) pharmacokinetic profiles (http://www.swissadme.ch/) (Daina et al. 2014, 2017; Daina and Zoete 2016; Al Azzam 2023), toxicity potential (https://biosig.lab.uq.edu.au/pkcsm/) (Pires et al. 2015; Al Azzam 2023), and molecular docking interactions. The tested compounds were selected based on GC-MS analysis, namely stigmast-4-e*n*-3-one, 4',6'-dimethoxy-2'-hydroxy-3-nitrochalcone, 2-(pyridi*n*-2-ylformamido) acetic acid, DL-alpha-tocopherol, and phytol.

For molecular docking, all test ligands were downloaded in their two-dimensional structures from PubChem (https://pubchem.ncbi.nlm.nih.gov) and then converted into 3D structures in PDB format using MarvinSketch© v6.0.0 software (ChemAxon Ltd). The reference ligand, alpha-acarbose and 5-chloro-1-(4-chlorobenzyl)-3-(phenylthio)-1H-indole-2-carboxylic acid, was obtained by separating it from the 2QMJ and 2Q5S receptors, respectively. All ligands were optimized and saved in pdbqt format using Autodock Tools v1.5.7 (The Scripps Research Institute). The maltase-glucoamylase receptor (2QMJ) and PPAR-γ receptor (2Q5S) were obtained from the Protein Data Bank (https://www.rcsb.org). Preparation was performed by removing water molecules and ligands, and the receptors were saved in PDB format. Hydrogen atoms were added to the polar groups, and Gasteiger charge calculations were performed using Autodock Tools. The receptors were then saved in PDBQT format.

Before performing molecular docking, several validations were conducted on the ligand binding site or binding region through grid box validation. This validation was carried out using AutoDock Vina (Trott and Olson 2010; Eberhardt et al. 2021) with coordinates of dimension $X = 24$, $Y = 24$, $Z = 24$, and a center of $X = 18.011$, $Y = 20.516$, $Z = 10.038$ for 2Q5S and RMSD = 0.825, and coordinates of dimension $X = 10$, $Y = 8$, $Z = 18$, and a center of $X = -21.727$, $Y = -6.323$, $Z = -5.280$ for 2QMJ and RMSD = 0.888. Docking analysis was performed using the Lamarckian Genetic Algorithm with 100 docking runs, and the best result was selected as the lowest binding energy. The protei*n*-ligand complexes and their molecular interactions were visualized using PyMOL (PyMOL Molecular Graphics System, version 2.5.8; Schrödinger, LLC), and two-dimensional visualization was performed using LigPlot+© v2.2.8 (Laskowski and Swindells 2011).

RESULTS AND DISCUSSION

Phytochemical test

A sample of the plant specimen has been identified in the Herbarium Wanariset (WAN) as *Macaranga depressa* Müll.Arg. forma strigosa Whitmore. Leaf samples were air-dried and macerated with *n*-hexane solvent. The obtained *n*-hexane extract was then used for further testing. Preliminary tests or phytochemical tests showed that the *n*-hexane extract of *M. depressa* leaves contained alkaloid, flavonoid, terpenoid/steroid, and tannin compounds, but the saponin test was negative (Table 1). These findings suggest the occurrence of no*n*-polar bioactive compounds that are predominantly soluble in no*n*-polar solvents, such as *n*-hexane.

Antimicrobial activity

The antimicrobial potential of the *n*-hexane extract of *M. depressa* leaves was tested against *Candida albicans*, *Escherichia coli*, *Staphylococcus aureus*, *Pseudomonas aeruginosa* (Table 2). All tested microorganisms exhibited sensitivity to the extract, indicating the presence of active compounds with antibacterial and antifungal properties. The highest inhibitory effect was observed against *P. aeruginosa*, followed by *S. aureus*, *E. coli*, and *C. albicans*. The inhibition zones in all replicates showed consistent values with relatively low variation. For *P. aeruginosa*, the inhibition zones ranged from 22.5 mm to 25.0 mm across replicates, suggesting that the extract is notably effective against Gram-negative bacteria, which are typically more resistant. Although *C. albicans* showed the smallest mean inhibition zone (18.0 mm), the result still demonstrates the antifungal activity of the *n*-hexane extract of *M. depressa* leaves. These findings support further investigation into the bioactive compounds responsible for this activity and their potential development as antimicrobial agents.

Phytochemical profiling by GC-MS analysis

To determine the chemical composition of the *n*-hexane extract of *M. depressa* leaves, GC-MS analysis was performed. The analysis revealed the presence of 31 compounds in the extract. Among these, five were the most abundant based on their peak area (Tables 3 and 4). The presence of various chemical constituents—particularly those known for their antimicrobial, antioxidant, or anti-inflammatory properties—may account for the biological activities observed in this study. Compounds such as terpenoids, hydrocarbons, esters, and fatty acid derivatives were among the major constituents identified.

Stigmast-4-e*n*-3-one is the compound with the largest chromatogram area, 32.76%, with a retention time of 31.667 minutes. This sterol compound has the molecular formula $C_{29}H_{48}O$ and a molecular weight of 412.7 g/mol. The second most abundant compound is 4′,6′-dimethoxy-2′-hydroxy-3-nitrochalcone, a nitro-substituted flavonoid derivative. Other major compounds include 2-(pyridi*n*-2-ylformamido) acetic acid, a nitroge*n*-containing heterocyclic acid; DL-alpha-tocopherol, known for its antioxidant properties; and phytol, a diterpene alcohol commonly found in the chlorophyll degradation pathway.

Table 1. Secondary metabolite profile of the *n*-hexane extract of *Macaranga depressa* leaves

Secondary metabolite	Test result
Alkaloid	+
Flavonoid	+
Saponin	-
Terpeneoid	+
Tannin	+

Note: +: Indicates presence, -: Indicates absence

Table 2. Inhibition zone diameter of the *n*-hexane extract of *Macaranga depressa* leaves

Isolate	Zone of inhibition (mm)			Average (mm)
	Replication 1	Replication 2	Replication 3	
Candida albicans	18.3	17.5	18.2	18.0±0.44
Control (+)	25.8	26.1	26.2	26.0±0.21
Escherichia coli	18.9	20.0	19.2	19.4±0.57
Control (+)	24.8	25.1	25.0	25.0±0.15
Pseudomonas aeruginosa	25.0	23.0	22.5	23.5±1.32
Control (+)	25.0	24.6	25.0	24.9±0.23
Staphylococcus aureus	20.8	21.7	21.0	21.2±0.47
Control (+)	22.8	23.5	23.1	23.1±0.35
Control (-)	0	0	0	0

Table 3. GC-MS analysis of the *n*-hexane extract of *Macaranga depressa* leaves

Peak	RT	Compound	Molecular formula	Molecular weight (g/mol)	Chromatogram peak area (%)
26	31.667	Stigmast-4-e*n*-3-one	$C_{29}H_{48}O$	412.70	32.76
20	28.521	4',6'-Dimethoxy-2'-hydroxy-3-nitro chalcone	$C_{17}H_{15}NO_6$	329.30	14.82
30	36.666	2-(Pyridi*n*-2-ylformamido) acetic acid	$C_8H_8N_2O_3$	180.16	7.58
19	28.367	DL-Alpha-Tocopherol	$C_{29}H_{50}O_2$	430.70	6.37
7	19.085	Phytol	$C_{20}H_{40}O$	296.50	4.58

Note: RT: Retention Time

Table 4. Compounds extracted from the *n*-hexane extract of *Macaranga depressa* leaves

Compounds	PubChem CID	Compound structure	2D structure
Compound 1: Stigmast-4-e*n*-3-one	5484202	CC[C@H](CC[C@@H](C)[C@H]1 CC[C@@H]2[C@@]1(CC[C@H]3 [C@H]2CCC4=CC(=O)CC[C@]34C)C)C(C)C	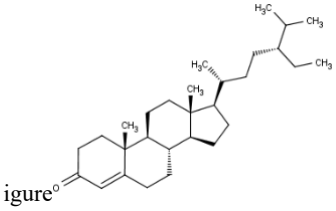
Compound 2: 4',6'-dimethoxy-2'-hydroxy-3-nitrochalcone	6063903	COC1=CC(=C(C(=C1)OC)C(=O)/C=C/C2=CC (=CC=C2)[N+](=O)[O-])O	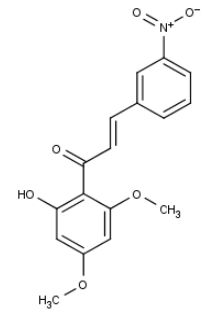
Compound 3: 2-(pyridi*n*-2-ylformamido) acetic acid	11788622	C1=CC=NC(=C1)C(=O)NCC(=O)O	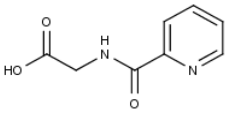
Compound 4: DL-alpha-tocopherol	2116	CC1=C(C2=C(CCC(O2)(C)CCCC(C)CCCC(C)CC CC(C)C)C(=C1O)C)C	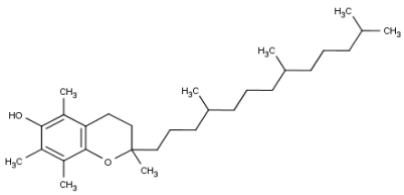
Compound 5: Phytol	5280435	C[C@@H](CCC[C@@H](C)CCC/C(=C/CO)/C)CC CC(C)C	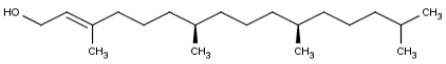

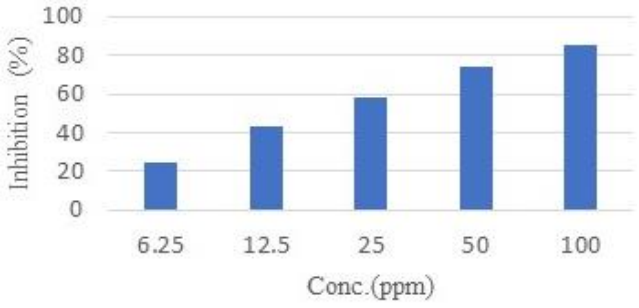

Figure 1. Inhibition activity α-glucosidase enzyme of the *n*-hexane extract of *Macaranga depressa* leaves

Antidiabetic activity

In addition to its potential as an antimicrobial agent, the extract of *M. depressa* leaves also exhibited antidiabetic activity. At a concentration of 17.561 ppm, the extract showed an α-glucosidase inhibitory effect of 50% (Table 5). The graph in Figure 1 shows that increasing concentration is proportional to the increase in the percentage of α-glucosidase enzyme inhibition activity. These results indicate the extract's potential within the moderate to strong activity category. This value is almost the same as the antidiabetic activity of the *n*-hexane fraction of *M. tanarius* leaves, which has an IC_{50} value of 12.46 ppm (Megawati et al. 2021). Cahyana et al. (2023) reported on the methanol extract of stem bark *M. mappa* that IC_{50} value was 7.204 ppm, the water fraction was 6.654 ppm, ethyl acetate was 26.897 ppm, butanol was 15.817 ppm and *n*-hexane provided the weakest inhibitory power with an IC_{50} value of 335.357 ppm. This indicates that the compounds contained in the polar fraction have better antidiabetic activity than the no*n*-polar fraction. Based on the data above, it can be stated that the *n*-hexane extract of *M. depressa* has more potential as an antidiabetic than the *n*-hexane fraction of *M. mappa*. The presence of bioactive lipophilic compounds, as identified by GC-MS, may contribute not only to the antimicrobial effect but also to the observed enzyme inhibition. Overall, these findings suggest that the *n*-hexane extract of *M. depressa* leaves possesses multiple bioactivities, supporting its potential application in the development of multifunctional herbal therapies.

To support the information on selected bioactive compounds and their role in antidiabetic activity, an in

silico study was conducted on five compounds chosen from the GC-MS analysis. These five compounds represent the most abundant bioactive candidates in the extract. The computational evaluation included analysis of drug-likeness (Table 6), ADME pharmacokinetic profiles (Table 7), toxicity potential (Table 8), and molecular interactions with selected protein targets to assess their therapeutic potential.

Table 5. Inhibition activity of α-glucosidase enzyme with $p<0.01$

Sample	IC_{50} (ppm)			Average (ppm)
	Replication 1	Replication 2	Replication 3	
Extract	17.318	18.104	17.261	17.561±0.471
Acarbose	0.006	0.006	0.006	0.006±0.000

Table 6. Drug-likeness prediction of the compounds from *n*-hexane extract of *Macaranga depressa* leaves

Compounds	Lipinski	Ghose	Veber	Egan	Muegge	Bioavailability score
Stigmast-4-e*n*-3-one	Pass	Fail	Pass	Fail	Fail	0.55
4',6'-Dimethoxy-2'-hydroxy-3-nitrochalcone	Pass	Pass	Pass	Pass	Pass	0.55
2-(Pyridi*n*-2-ylformamido) acetic acid	Pass	Pass	Pass	Pass	Fail	0.56
DL-Alpha-Tocopherol	Pass	Fail	Fail	Fail	Fail	0.55
Phytol	Pass	Fail	Fail	Fail	Fail	0.55

Table 7. ADME pharmacokinetic properties of the compounds from *n*-hexane extract of *Macaranga depressa* leaves

Parameters	Compound 1	Compound 2	Compound 3	Compound 4	Compound 5
Absorption					
Water solubility (log mol/L)	-6.212	-5.025	-1.510	-6.901	-7.535
Caco2 permeability (log Papp in 10^{-6} cm/s)	1.213	1.183	0.676	1.345	1.399
Intestinal absorption (human)	98.556	89.317	87.806	89.782	90.643
Skin permeability (log Kp)	-2.708	-2.719	-2.735	-2.683	-2.631
P-glycoprotein substrate	No	No	No	No	No
P-glycoprotein I inhibitor	No	Yes	No	No	No
P-glycoprotein II inhibitor	Yes	Yes	No	Yes	No
Distribution					
VDss (human) (log L/kg)	-0.141	-0.455	-0.97	0.709	0.385
Fraction unbound (human)	0	0	0.74	0	0
BBB permeability (log BB)	0.847	-0.757	-0.253	0.876	0.793
CNS permeability (log PS)	-1.358	-2.442	-3.044	-1.669	-1.527
Metabolism					
CYP2D6 substrate	No	No	No	No	No
CYP3A4 substrate	Yes	Yes	No	Yes	Yes
CYP1A2 inhibitor	No	Yes	No	No	Yes
CYP2C19 inhibitor	No	Yes	No	Yes	No
CYP2C9 inhibitor	No	Yes	No	No	No
CYP2D6 inhibitor	No	No	No	No	No
CYP3A4 inhibitor	No	No	No	No	No
Excretion					
Total Clearance (log mL/min/Kg)	0.560	0.313	0.247	0.794	1.686
Renal OCT2 substrate	No	No	No	No	No

Note: OCT2: Organic Cation Transporter 2, BBB: Blood-Brain Barrier, CNS: Central Nervous System, VDss: Steady-state Volume of Distribution

Table 8. Toxicity properties of the compounds from *n*-hexane extract of *Macaranga depressa* leaves

Parameters	Compound 1	Compound 2	Compound 3	Compound 4	Compound 5
AMES toxicity	No	Yes	No	No	No
Max. tolerated dose (human) (log mg/kg/day)	-0.458	0.065	1.808	0.775	-0.301
hERG I inhibitor	No	No	No	No	No
hERG II inhibitor	Yes	No	No	Yes	Yes
Oral rat acute toxicity (LD50) (mol/kg)	2.531	2.126	1.812	2.072	1.848
Oral rat chronic toxity (LOAEL) (log mg/kg_bw/day)	0.871	1.886	2.065	1.987	1.232
Hepatotoxicity	No	No	Yes	No	No
Skin sensitization	No	No	No	No	Yes
Tetrahymena pyriformis toxicity (log µg/L)	0.325	0.52	0.259	1.017	1.714
Minnow toxicity (log mM)	-2.556	-1.604	3.272	-3.324	-1.137

In terms of drug-like properties, only 4′,6′-dimethoxy-2′-hydroxy-3-nitrochalcone met all five drug-likeness criteria (Lipinski, Ghose, Veber, Egan, and Muegge) with a bioavailability score of 0.55. The other compounds passed Lipinski's rule but failed at least one of the other rules. 2-(Pyridi*n*-2-ylformamido) acetic acid passed through four filters but failed Muegge's criteria. ADME analysis revealed that all five compounds showed a high intestinal absorption (>87%) and were not substrates for P-glycoprotein, indicating good oral bioavailability potential. Predicted skin permeability (log Kp) values for all tested compounds were less than -2.5, indicating poor dermal penetration. Regarding distribution, DL-alpha-tocopherol and phytol showed positive Blood-Brain Barrier (BBB) permeability values (>0.7), indicating potential CNS accessibility. None of the compounds were CYP2D6 substrates, but three were predicted to be CYP3A4 substrates, suggesting susceptibility to hepatic metabolism. Toxicity profiles revealed that only 4′,6′-dimethoxy-2′-hydroxy-3-nitrochalcone was positive for Ames mutagenicity, whereas 2-(pyridi*n*-2-ylformamido) acetic acid was predicted to be hepatotoxic. None of the compounds inhibited hERG I, but three were predicted to be hERG II inhibitors, indicating some potential cardiac toxicity. LD50 and LOAEL values varied among the compounds, with 2-(pyridi*n*-2-ylformamido) acetic acid having the highest oral safety margin.

Binding affinity analysis

Table 9 presents the results of molecular docking analysis between the selected compounds and the receptors Human Maltase-Glucoamylase (PDB ID: 2QMJ) and Human PPAR-γ (PDB ID: 2Q5S). The results revealed that 4′,6′-dimethoxy-2′-hydroxy-3-nitrochalcone showed the strongest affinity for Human Maltase-Glucoamylase (-8.1 kcal/mol), surpassing the native ligand alpha-acarbose (-7.2 kcal/mol), which serves as an antidiabetic drug. Meanwhile, stigmast-4-e*n*-3-one and DL-alpha-tocopherol also showed promising affinities for Human Maltase-Glucoamylase, with values of -7.5 and -6.0 kcal/mol, respectively. Against PPAR-γ, stigmast-4-e*n*-3-one exhibited the highest binding affinity among the tested compounds (-9.6 kcal/mol), followed by DL-alpha-tocopherol and 4′,6′-dimethoxy-2′-hydroxy-3-nitrochalcone; however, these affinity values did not exceed that of the native ligand NZA. Additionally, the docking results suggest that compounds in the *n*-hexane extract of *M. depressa* leaves are effective in interacting with the Human Maltase-Glucoamylase receptor.

Molecular interaction analysis

In the Human Maltase-Glucoamylase enzyme, 4′,6′-dimethoxy-2′-hydroxy-3-nitrochalcone interacts via hydrogen bonding with residues such as His600 and engages in hydrophobic contacts with Trp406—both of which are crucial for stabilizing the substrate. As reflected in Table 10, this compound demonstrates a higher binding affinity than the native ligand. These findings reinforce the identification of Human Maltase-Glucoamylase as the principal target receptor for the bioactive compounds found in the *M. depressa* leaf *n*-hexane extract. Regarding PPAR-γ, the active molecules form interactions with amino acid residues including Cys285, Ile341, and Leu340, which are known to contribute to ligand recognition (Priya et al. 2024). Several compounds exhibit both hydrogen bonding and hydrophobic interactions at the binding site. Notably, stigmast-4-e*n*-3-one only participates in hydrophobic interactions and lacks hydrogen bonding, likely due to its predominantly no*n*-polar methyl group composition.

Discussion

The phytochemical profile of the *n*-hexane extract of *M. depressa* leaves contained several classes of secondary metabolites with well-known pharmacological activities. Alkaloids, flavonoids, terpenoids, and tannins are all recognized for antimicrobial, antioxidant, and anti-inflammatory effects. (Farhadi et al. 2019; Ullah et al. 2020; Roy et al. 2022; Gonfa et al. 2023; Zouine et al. 2024). Alkaloids are known to disrupt microbial membranes and interfere with nucleic acid synthesis (Yan et al. 2021; Karunakaran et al. 2022; Thawabteh et al. 2024), while flavonoids can bind to bacterial membranes and inhibit essential enzymes (Vaou et al. 2021; De Rossi et al. 2025; Liu et al. 2025). Terpenoids, typically soluble in no*n*-polar solvents, may destabilize microbial membranes and interfere with quorum sensing (Sharma et al. 2020). Tannins act mainly through protein precipitation and enzyme inhibition (Huang et al. 2024). The absence of saponins, usually extracted with polar solvents, reflects the selectivity of *n*-hexane for lipophilic metabolites.

Table 9. Binding affinity from the docking analysis

Compounds	Binding affinity, kcal/mol	
	Human Maltase-Glucoamylase (PDB ID: 2QMJ)	**Human PPAR-γ (PDB ID: 2Q5S)**
Native ligand	alpha-acarbose = -7.2 [RMSD = 0.825]	NZA = -10.9 [RMSD = 0.888]
Stigmast-4-e*n*-3-one	-7.5	-9.6
4',6'-Dimethoxy-2'-hydroxy-3-nitrochalcone	-8.1	-9.1
2-(Pyridi*n*-2-ylformamido) acetic acid	-5.5	-6.9
DL-Alpha-Tocopherol	-6.0	-9.1
Phytol	-5.8	-7.3

Note: NZA: 5-chloro-1-(4-chlorobenzyl)-3-(phenylthio)-1H-indole-2-carboxylic acid

Table 10. Molecular interactions of antidiabetic compounds

Compounds	Ligand interaction	
	Human Maltase-Glucoamylase (PDB ID: 2QMJ)	**Human PPAR-γ (PDB ID: 2Q5S)**
Stigmast-4-e*n*-3-one	Hydrophobics: Tyr 299, Asp 327, Trp 406, Ala 576, Thr 205, Thr 544, Asp 542, Phe 575	Hydrophobics: Val 339, Leu 330, Gly 284, Cys 285, Leu 255, Ile 281, Met 348, Ile 249, Gly 258, Glu 259, Leu 340, Ser 342, Ile 341, Arg 288, Leu 333
4',6'-Dimethoxy-2'-hydroxy-3-nitrochalcone	Hydrophobics: Asp 327, Tyr 299, Trp 406, Tyr 605, Ala 576, Thr 205, Phe 575, Asp 542, Asp 443, Trp 441, Trp 539 Hydrogen bond: His 600	Hydrophobics: Leu 228, Met 329, Val 339, Leu 330, Cys 285, Gly 284, Ile 341, Ala 292, Leu 333 Hydrogen bond: Arg 288, Ile 326
2-(Pyridi*n*-2-ylformamido) acetic acid	Hydrophobics: Trp 539, Trp 441, Asp 542, Asp 443, Met 444, Trp 406, Tyr 299, Phe 575 Hydrogen bond: His 600, Arg 526	Hydrophobics: Leu 333, Leu 228, Ile 341 Hydrogen bond: Glu 343, Arg 288, Ser 342
DL-Alpha-Tocopherol	Hydrophobics: Thr 205, Asp 203, Asp 542, Trp 406, Asp 327, Tyr 299, Phe 575	Hydrophobics: Ala 292, Ile 296, Ser 289, Ile 326, Arg 288, Met 329, Met 364, Met 348, Cys 285, Gly 284, Ile 341, Leu 340, Leu 333, Ser 342, Leu 228, Leu 330, Glu 295 Hydrogen bond: Ile 281
Phytol	Hydrophobics: Asp 203, Thr 205, Phe 575, Tyr 299, Ile 364, Met 444, Ile 328, Asp 542, Trp 441, Asp 327, Ala 576, Thr 204 Hydrogen bond: Asp 443, Trp 406	Hydrophobics: Glu 295, Ala 292, Leu 228, Leu 333, Arg 288, Ile 341, Glu 343, Cys 285, Ser 289, Leu 330, Ile 326, Ile 296, Met 329 Hydrogen bond: Leu 340

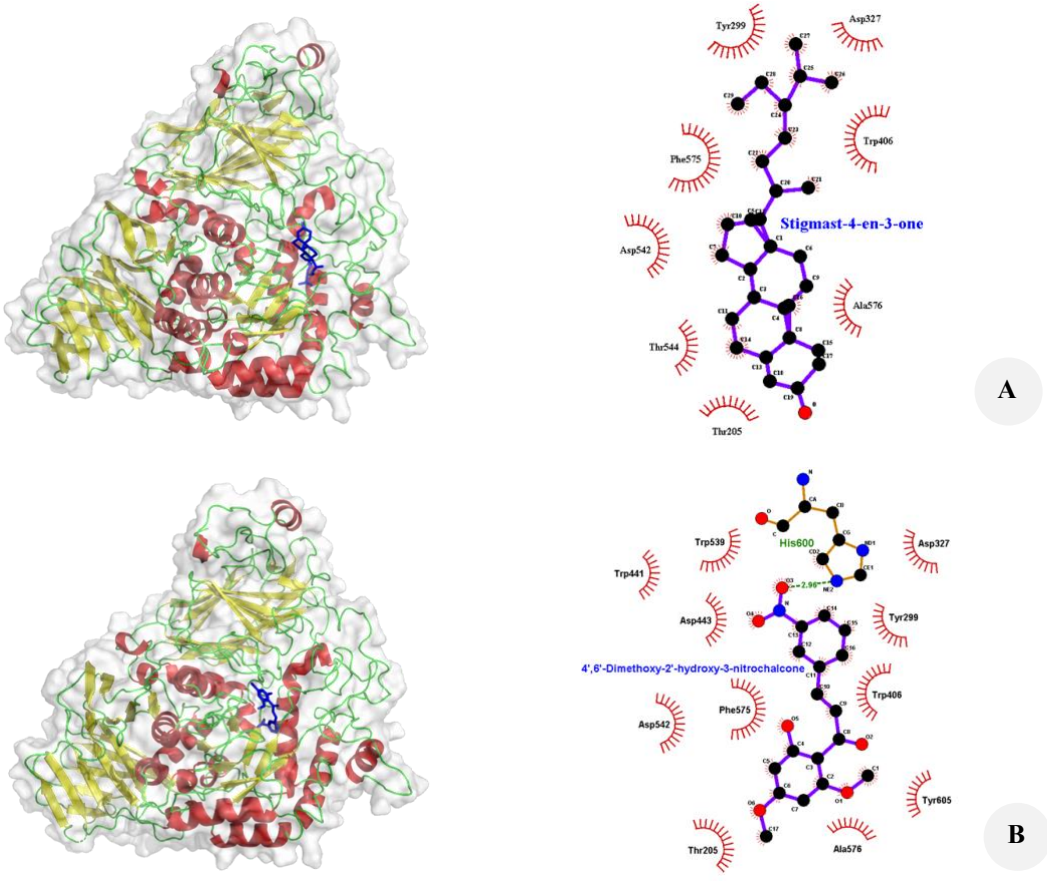

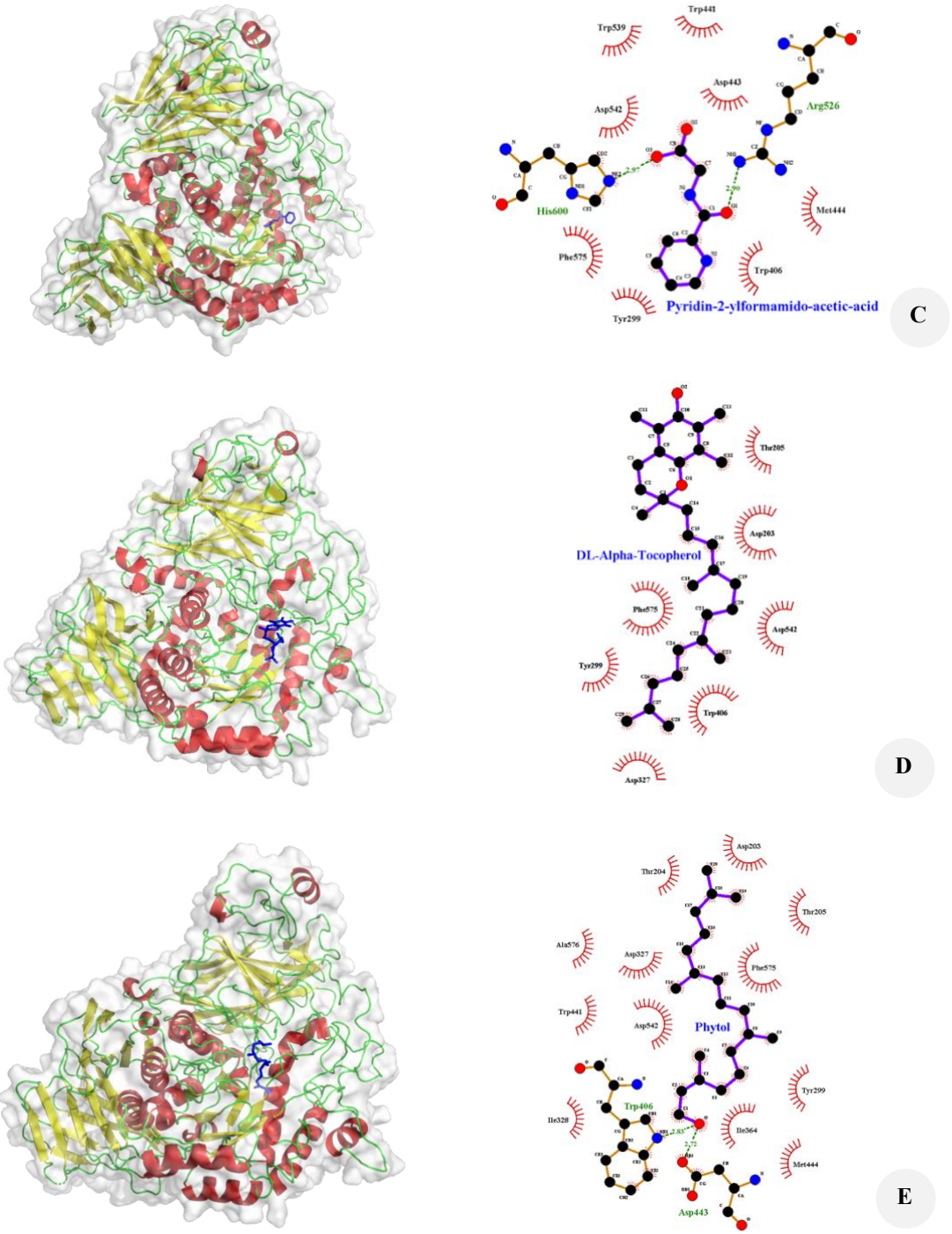

Figure 2. Molecular interactions of compounds from *Macaranga depressa* leaves *n*-hexane extract with Human Maltase-Glucoamylase (PDB ID: 2QMJ). A. Stigmast-4-en-3-one, B. 4',6'-Dimethoxy-2'-hydroxy-3-nitrochalcone, C. 2-(Pyridin-2-ylformamido) acetic acid, D. DL-Alpha-Tocopherol, E. Phytol

These phytochemicals correspond with the extract's broad antimicrobial activity. The *n*-hexane extract of *M. depressa* leaves exhibited strong antimicrobial activity against both Gram-positive and Gram-negative bacteria, as well as fungi, *C. albicans*. The most sensitive strain to this extract was *P. aeruginosa*, a Gram-negative bacterium often associated with antibiotic resistance. This suggests that the compounds present in the extract may disrupt the integrity of the outer membrane or inhibit vital enzymes of pathogens that are typically resistant to antibiotics (Khameneh et al. 2021). The observed antimicrobial activity is attributed to the presence of lipophilic secondary metabolites detected in the extract (Table 1). Terpenoids and flavonoids have been reported to inhibit microbial growth by disrupting membrane integrity, generating Reactive Oxygen Species (ROS), or inhibiting nucleic acid

synthesis (Zore et al. 2011; Rodríguez et al. 2023). In addition to its activity against Gram-negative bacteria, the extract also exhibited inhibitory effects against *S. aureus*, a Gram-positive pathogen implicated in skin and soft tissue infections. This indicates that the *n*-hexane extract of *M. depressa* leaves is effective against a broad spectrum of microbes. The presence of flavonoids and tannins, which could bind to microbial proteins, may contribute to this activity by deactivating microbial adhesins and enzymes. Furthermore, antifungal activity against *C. albicans* supports the broad-spectrum potential of the extract. Lipophilic flavonoids and terpenoids have been reported to exert fungistatic or fungicidal effects by interfering with ergosterol biosynthesis and membrane permeability (Haque et al. 2016; Al Aboody and Mickymaray 2020; Medeiros et al. 2022; Vishwakarma et al. 2024). Collectively, the observed antimicrobial effects support the ethnomedicinal use of *M. depressa* and suggest that its bioactive compounds may serve as potential raw materials for the development of new antimicrobial agents, especially considering the growing problem of antibiotic resistance. To the best of our knowledge, this is the first integrated study that simultaneously characterizes the phytochemical profile, antimicrobial activity, and in silico molecular interactions of *M. depressa.*

The *n*-hexane extract of *M. depressa* leaves exhibited significant inhibitory activity against the α-glucosidase enzyme, with an inhibition percentage of 85.53% at a concentration of 100.00 ppm (Figure 1). These results indicate that the extract contains bioactive compounds capable of modulating carbohydrate metabolism by delaying the breakdown of complex sugars into glucose. Inhibition of α-glucosidase is a recognized therapeutic approach to managing postprandial hyperglycemia in patients with type 2 diabetes mellitus (Joshi et al. 2015; Dirir et al. 2021). The lipophilic nature of the extract suggests the involvement of no*n*-polar phytochemicals, such as terpenoids, fatty acids, and sterols, which have been reported to possess antidiabetic properties. Compounds identified through GC-MS analysis, particularly long-chain hydrocarbons, esters, and triterpenoids, are associated with enzyme inhibition and the regulation of glucose metabolism. These compounds are believed to inhibit α-glucosidase by either occupying its active site or inducing conformational changes that reduce its catalytic efficiency. The inhibitory activity of *M. depressa* extract against α-glucosidase compared to the *n*-hexane fraction of *Macaranga tanarius* leaves was slightly lower, but against petroleum ether extracts from *M. hosei* and *M. constricta* leaves it was more active (Salleh et al. 2017; Megawati et al. 2021). Thus, the present findings reinforce the potential of *M. depressa* as a natural source of antidiabetic agents. Moreover, the multifunctional nature of the extract—evident from its antimicrobial and antidiabetic properties—may provide additional therapeutic benefits, particularly for diabetic patients who are more susceptible to infections due to immune dysregulation. These dual bioactivities make *M. depressa* an attractive candidate for further pharmacological investigation and drug development.

The inhibitory effect can be mechanistically linked to several major phytochemicals identified by GC-MS. The GC-MS profile of the *n*-hexane extract of *M. depressa* leaves revealed a diverse phytochemical composition. The predominance of stigmast-4-e*n*-3-one, a steroidal compound, is noteworthy given its reported antimicrobial and anti-inflammatory properties (Sahidin et al. 2019; Nyalo et al. 2023; Razafindrakoto et al. 2024). Its structural similarity to phytosterols suggests potential membrane-disrupting activity, which may contribute to the antimicrobial effects observed in previous assays, while its phytosterol-like scaffold has also been linked to modulation of glucose and lipid metabolism through PPAR-γ, supporting a possible role in enhancing insulin sensitivity. The presence of 4′,6′-dimethoxy-2′-hydroxy-3-nitrochalcone is also of interest due to the pharmacological versatility of the chalcone scaffold, which has been associated with antibacterial, antifungal, and anticancer activities (Bhathiwal et al. 2022; Mendez-Callejas et al. 2024). Nitro-substituted chalcones have been shown to increase lipophilicity and enhance microbial membrane permeability, which may explain their effectiveness against both Gram-positive and Gram-negative bacteria. Importantly, chalcones are also well-established α-glucosidase inhibitors, and the α,β-unsaturated ketone moiety present in this compound enables it to bind to the catalytic site of glycosidases, thereby contributing to the observed antidiabetic effect. DL-alpha-tocopherol, an isoform of vitamin E, is widely recognized for its antioxidant properties. However, recent studies have also reported its role in modulating immune responses and enhancing the efficacy of antimicrobial agents (Andrade et al. 2014; Naguib and Valvano 2018; Hartmann et al. 2020). Beyond its antimicrobial support, tocopherol has been associated with improved insulin action and protection of pancreatic β-cells from oxidative stress, providing an indirect mechanism for glycemic control. Similarly, phytol has been reported to possess antimicrobial, antitumor, and anti-inflammatory activities (Lee et al. 2016; Islam et al. 2018, 2020). In the context of diabetes, phytol has also been linked to antihyperglycemic and hypolipidemic effects, potentially through modulation of glucose uptake and regulation of metabolic enzymes. Furthermore, 2-(pyridi*n*-2-ylformamido) acetic acid was also detected. Although it has not been widely studied, its structural features suggest potential bioactivity due to the presence of a heterocyclic nitrogen and a carboxamide functional group, both of which are recognized pharmacophores in various drug classes. Overall, the *n*-hexane extract of *M. depressa* leaves demonstrates promising α-glucosidase inhibition, though less potent than *Macaranga tanarius* and *Moringa oleifera* as seen in Table 11.

Considering their potential bioactivity and abundance as indicated by the GC-MS analysis, the compounds were further evaluated through a series of in silico analyses. These analyses serve as a preliminary drug screening process, assessing drug-likeness based on Lipinski's Rule of Five, ADME (Absorption, Distribution, Metabolism, and Excretion) property prediction, and toxicity risk. Molecular docking was also performed on all five compounds to support the hypothesis regarding their potential antidiabetic activity. This computational approach provides both predictive and confirmatory insights into the pharmacological behavior of the molecules.

Table 11. Inhibition values comparison with previous studies

Plant	IC_{50} against the α-glucosidase enzyme (ppm)	Reference
n-hexane extract *Macaranga depressa* leaves	17.561±0.471	This study
n-hexane fraction of *Macaranga tanarius* leaves	12.46	Megawati et al. (2021)
petroleum eter extract of *Macaranga hosei* leaves	25.30	Salleh et al. (2017)
petroleum eter extract of *Macaranga constricta* leaves	237.6	Salleh et al. (2017)
n-hexane extract of *Moringa oleifera* leaves	3.43±0.06	Magaji et al. (2020)

In silico analysis of 4′,6′-dimethoxy-2′-hydroxy-3-nitrochalcone revealed that this compound is a promising candidate due to its ability to meet five major drug-likeness criteria. It has high potential for oral bioavailability, membrane permeability, and favorable physicochemical properties, making it suitable for drug development. The ADME (Absorption, Distribution, Metabolism, and Excretion) prediction further supported its potential. All compounds demonstrated high predicted intestinal absorption (>87%), which is a critical parameter for the development of orally administered drugs. Moreover, none of the compounds were identified as P-glycoprotein substrates, suggesting a lower likelihood of efflux-related resistance or reduced bioavailability, common issues in drug transport mechanisms. The predicted Blood-Brain Barrier (BBB) permeability of DL-alpha-tocopherol and phytol suggests possible Central Nervous System (CNS) bioactivity, warranting further investigation into their potential neuroprotective or CNS-related therapeutic roles. Metabolic profiling indicated that most of the compounds are likely substrates of CYP3A4, highlighting their susceptibility to hepatic metabolism and raising the possibility of drug-drug interactions (Guengerich 2008). In contrast, 2-(pyridi*n*-2-ylformamido) acetic acid was not predicted to be a CYP3A4 substrate, although its potential hepatotoxicity may limit its therapeutic applicability. Additionally, the presence of hERG II inhibition in some compounds necessitates caution due to possible cardiotoxic effects, despite the absence of hERG I inhibition, which is more strongly associated with serious cardiac arrhythmias (Redfern et al. 2003). Interestingly, although stigmast-4-e*n*-3-one and phytol showed suboptimal drug-likeness based on several filters, both compounds were predicted to be no*n*-mutagenic and no*n*-hepatotoxic with acceptable safety profiles. This suggests that they could be structurally optimized or formulated to enhance their drug-like properties.

The docking results demonstrated that 4′,6′-dimethoxy-2′-hydroxy-3-nitrochalcone is a potent inhibitor of human maltase-glucoamylase, with a binding affinity superior to acarbose, a clinically used α-glucosidase inhibitor. These findings are consistent with the ADME and Lipinski's Rule analyses, which indicated that 4′,6′-dimethoxy-2′-hydroxy-3-nitrochalcone satisfies all five drug-likeness criteria. Previous studies have highlighted that the α,β-unsaturated ketone moiety present in chalcones contributes to α-glucosidase inhibition by interacting with key active-site residues such as His600 and Trp406. In addition, stigmast-4-e*n*-3-one and DL-alpha-tocopherol exhibited high binding affinities toward PPAR-γ. Although their affinities were lower than the native inhibitor, these compounds may function as partial agonists, offering potential advantages over full agonists, such as reduced side effects (Soccio et al. 2014). These in silico results support the concept of dual inhibition of simultaneously targeting human maltase-glucoamylase and PPAR-γ as a promising strategy for diabetes therapy, as it both lowers postprandial glucose levels and improves insulin sensitivity. Overall, these findings emphasize the potential of chalcone derivatives and phytosterols as multitarget antidiabetic agents through modulation of maltase-glucoamylase and PPAR-γ. Therefore, it is necessary to isolate the compounds in the *n*-hexane extract of *M. depressa* leaves to obtain pure compounds and to test these pure compounds for antidiabetic and antibacterial activity both in vitro and in vivo.

In conclusion, the *n*-hexane extract of *M. depressa* leaves exhibits considerable bioactive potential, as reflected by its broad-spectrum antimicrobial effects and notable α-glucosidase inhibitory activity, with molecular docking results further supporting strong interactions between its major compounds and both α-glucosidase and PPAR-γ receptors. Nevertheless, the current findings are constrained by the use of a crude extract, where synergistic or antagonistic interactions among diverse metabolites may obscure the precise contribution of individual bioactive compounds. Moreover, the evidence so far is limited to in vitro assays and computational modeling, without accompanying in vivo pharmacological or toxicological validation to confirm efficacy, bioavailability, and safety in biological systems. Future investigations should therefore prioritize the isolation, purification, and structural characterization of the most active constituents, followed by comprehensive in vivo studies to elucidate their pharmacokinetics, therapeutic potential, and safety profiles.

ACKNOWLEDGEMENTS

We gratefully acknowledge funding from Universitas Lambung Mangkurat, South Kalimantan, Indonesia, through the 2024 BLU DIPA (No. SP DIPA-023.17.2.677518/2024).

REFERENCES

Al Aboody MS, Mickymaray S. 2020. Anti-fungal efficacy and mechanisms of flavonoids. Antibiotics 9: 45. DOI: 10.3390/antibiotics9020045.

Al Azzam K. 2023. SwissADME and pkCSM webservers predictors: An integrated online platform for accurate and comprehensive predictions for in silico ADME/T properties of artemisinin and its derivatives. Complex Use Min Resour 325: 14-21. DOI: 10.31643/2023/6445.13.

Aldughaylibi FS, Raza MA, Naeem S, Rafi H, Alam MW, Souayeh B, Farhan M, Aamir M, Zaidi N, Mir TA. 2022. Extraction of bioactive

compounds for antioxidant, antimicrobial, and antidiabetic applications. Molecules 27 (18): 5935. DOI: 10.3390/molecules27185935.

Andrade JC, Morais-Braga MFB, Guedes GMM, Tintino SR, Freitas MA, Menezes IRA, Coutinho HDM. 2014. Enhancement of the antibiotic activity of aminoglycosides by alpha-tocopherol and other cholesterol derivatives. Biomed Pharmacother 68 (8): 1065-1069. DOI: 10.1016/j.biopha.2014.10.011.

Bailey CJ. 2017. Metformin: Historical overview. Diabetologia 60 (9): 1566-1576. DOI: 10.1007/s00125-017-4318-z.

Bhathiwal AS, Bendi A, Tiwari A. 2022. A study on synthesis of benzodiazepine scaffolds using biologically active chalcones as precursors. J Mol Struct 1258: 132649. DOI: 10.1016/j.molstruc.2022.132649.

Cahyana AH, Liandi AR, Wicaksono SS, Darmawan A. 2023. Biological activities of extracts and secondary metabolite of *Macaranga mappa* bark as an antidiabetic by α-glucosidase inhibitor, antioxidant, and cytotoxicity. Rasayan J Chem 16 (1): 290-296. DOI: 10.31788/RJC.2023.1618029.

Daina A, Michielin O, Zoete V. 2014. iLOGP: A simple, robust, and efficient description of *n*-octanol/water partition coefficient for drug design using the GB/SA approach. J Chem Inf Model 54 (12): 3284-3301. DOI: 10.1021/ci500467k.

Daina A, Michielin O, Zoete V. 2017. SwissADME: A free web tool to evaluate pharmacokinetics, drug-likeness and medicinal chemistry friendliness of small molecules. Sci Rep 7: 42717. DOI: 10.1038/srep42717.

Daina A, Zoete V. 2016. A BOILED-Egg to predict gastrointestinal absorption and brain penetration of small molecules. ChemMedChem 11 (11): 1117-1121. DOI: 10.1002/cmdc.201600182.

De Rossi L, Rocchetti G, Lucini L, Rebecchi A. 2025. Antimicrobial potential of polyphenols: Mechanisms of action and microbial responses—A narrative review. Antioxidants 14 (2): 200. DOI: 10.3390/antiox14020200.

Dilworth L, Facey A, Omoruyi F. 2021. Diabetes mellitus and its metabolic complications: the role of adipose tissues. Intl J Mol Sci 22 (14): 7644. DOI: 10.3390/ijms22147644.

Dirir AM, Daou M, Yousef AF, Yousef LF. 2021. A review of alpha-glucosidase inhibitors from plants as potential candidates for the treatment of type 2 diabetes. Phytochem Rev 21 (4): 1049-1079. DOI: 10.1007/s11101-021-09773-1.

Eberhardt J, Santos-Martins D, Tillack AF, Forli S. 2021. AutoDock Vina 1.2.0: New docking methods, expanded force field, and Python bindings. J Chem Inf Model 61: 3891-3898. DOI: 10.1021/acs.jcim.1c00203.

Etsassala NGER, Badmus JA, Marnewick JL, Iwuoha EI, Nchu F, Hussein AA. 2020. Alpha-glucosidase and alpha-amylase inhibitory activities, molecular docking, and antioxidant capacities of *Salvia aurita* constituents. Antioxidants 9: 1149. DOI: 10.3390/antiox9111149.

Farhadi F, Khameneh B, Iranshahi M, Iranshahy M. 2019. Antibacterial activity of flavonoids and their structure-activity relationship: An update review. Phytother Res 33 (1): 13-40. DOI: 10.1002/ptr.6208.

Fonseca-Correa JI, Correa-Rotter R. 2021. Sodium-glucose cotransporter 2 inhibitors mechanisms of action: A review. Front Med 8: 777861. DOI: 10.3389/fmed.2021.777861.

Gizaw A, Marami LM, Teshome I, Sarba EJ, Admasu P, Babele DA, Dilba GM, Bune WM, Bayu MD, Tadesse M, Abdisa K. 2022. Phytochemical screening and in vitro antifungal activity of selected medicinal plants against *Candida albicans* and *Aspergillus niger* in West Shewa Zone, Ethiopia. Adv Pharmacol Pharm Sci 2022: 3299146. DOI: 10.1155/2022/3299146.

Gonfa YH, Tessema FB, Bachheti A, Rai N, Tadesse MG, Singab AN, Chaubey KK, Bachheti RK. 2023. Anti-inflammatory activity of phytochemicals from medicinal plants and their nanoparticles: A review. Curr Res Biotechnol 6: 100152. DOI: 10.1016/j.crbiot.2023.100152.

Guengerich FP. 2008. Cytochrome P450 and chemical toxicology. Chem Res Toxicol 21 (1): 70-83. DOI: 10.1021/tx700079z.

Haque E, Irfan S, Kamil M, Sheikh S, Hasan A, Ahmad A, Lakshmi V, Nazir A, Mir SS. 2016. Terpenoids with antifungal activity trigger mitochondrial dysfunction in *Saccharomyces cerevisiae.* Microbiology 85: 436-443. DOI: 10.1134/S0026261716040093.

Hartmann MS, Mousavi S, Bereswill S, Heimesaat MM. 2020. Vitamin E as promising adjunct treatment option in the combat of infectious diseases caused by bacterial including multi-drug resistant pathogens—results from a comprehensive literature survey. Eur J Microbiol Immunol 10 (4): 193-201. DOI: 10.1556/1886.2020.00020.

Hendriyani I, Safwan S, Ittiqo DH, Fitriana Y, Wahid AR. 2024. Uji aktivitas antibakteri dan antijamur fraksi aseton, etil asetat, dan air pada tanaman apu-apu (*Pistia stratiotes*). Lumbung Farmasi: Jurnal Ilmu Kefarmasian 5: 114-118. DOI: 10.31764/lf.v5i2.14591. [Indonesian]

Huang J, Zaynab M, Sharif Y, Khan J, Al-Yahyai R, Sadder M, Ali M, Alarab SR, Li S. 2024. Tannins as antimicrobial agents: understanding toxic effects on pathogens. Toxicon 247: 107812. DOI: 10.1016/j.toxicon.2024.107812.

Islam MT, Ali ES, Uddin SJ et al. 2018. Phytol: A review of biomedical activities. Food Chem Toxicol 121: 82-94. DOI: 10.1016/j.fct.2018.08.032.

Islam MT, Ayatollahi SA, Zihad SMNK, Sifat N, Khan MR, Paul A, Salehi B, Islam T, Mubarak MS, Martins N, Sharifi-Rad J. 2020. Phytol anti-inflammatory activity: Pre-clinical assessment and possible mechanism of action elucidation. Cell Mol Biol 66 (4): 264-269. DOI: 10.14715/cmb/2020.66.4.31.

Joshi SR, Standl E, Tong N, Shah P, Kalra S, Rathod R. 2015. Therapeutic potential of α-glucosidase inhibitors in type 2 diabetes mellitus: An evidence-based review. Expert Opin Pharmacother 16 (13): 1959-1981. DOI: 10.1517/14656566.2015.1070827.

Kamso VFK, Fotso CCS, Mbekou IMK, Tousssie BT, Lenta BN, Boyom FF, Sewald N, Frese M, Ngadjui BT, Fotso GW. 2022. Chemical constituents of *Macaranga occidentalis*, antimicrobial and chemophenetic studies. Molecules 27 (24): 8820. DOI: 10.3390/molecules27248820.

Karunakaran T, Ngew KZ, Zailan AAD, Jong VYM, Bakar MHA. 2022. The chemical and pharmacological properties of mitragynine and its diastereomers: An insight review. Front Pharmacol 13: 805986. DOI: 10.3389/fphar.2022.805986.

Khameneh B, Eskin NAM, Iranshahy M, Fazly Bazzaz BS. 2021. Phytochemicals: A promising weapon in the arsenal against antibiotic-resistant bacteria. Antibiotics 10 (9): 1044. DOI: 10.3390/antibiotics10091044.

Khanal S. 2021. Qualitative and quantitative phytochemical screening of *Azadirachta indica* Juss. plant parts. Intl J Appl Sci Biotechnol 9 (2): 122-127. DOI: 10.3126/ijasbt.v9i2.38050.

Laskowski RA, Swindells MB. 2011. LigPlot+: Multiple ligand-protein interaction diagrams for drug discovery. J Chem Inf Model 51 (10): 2778-2786. DOI: 10.1021/ci200227u.

Lee W, Woo E-R, Lee DG. 2016. Phytol has antibacterial property by inducing oxidative stress response in *Pseudomonas aeruginosa*. Free Radic Res 50 (12): 1309-1318. DOI: 10.1080/10715762.2016.1241395.

Liu Y, Zhu J, Liu Z, Zhi Y, Mei C, Wang H. 2025. Flavonoids as promising natural compounds for combating bacterial infections. Intl J Mol Sci 26 (6): 2455. DOI: 10.3390/ijms26062455.

Magaji UF, Sacan O, Yanardag R. 2020. Alpha amylase, alpha glucosidase and glycation inhibitory activity of *Moringa oleifera* extracts. S Afr J Bot 128: 225-230. DOI: 10.1016/j.sajb.2019.11.024.

Masyudi, Hanafiah M, Rinidar, Usman S, Marlina. 2022. Phytochemical screening and GC-MS analysis of bioactive compounds of *Blumea balsamifera* leaf extracts from South Aceh, Indonesia. Biodiversitas 23 (3): 1344-1352. DOI: 10.13057/biodiv/d230319.

Medeiros CIS, de Sousa MNA, Filho GGA, Freitas FOR, Uchoa DPL, Nobre MSC, Bezerra ALD, Rolim LADMM, Morais AMB, Nogueira TBSS, Nogueira RBSS, Filho AAO, Lima EO. 2022. Antifungal activity of linalool against fluconazole-resistant clinical strains of vulvovaginal *Candida albicans* and its predictive mechanism of action. Braz J Med Biol Res 55: e11831. DOI: 10.1590/1414-431X2022E11831.

Megawati, Hariyanti, Pebriani R, Fajriah S. 2021. Inhibition activity of α-glucosidase enzyme, phenolic content and toxicity of Mara (*Macaranga tanarius* (L.) Mull. Arg) leaf. IOP Conf Ser: Mater Sci Eng 1011: 012016. DOI: 10.1088/1757-899X/1011/1/012016.

Mendez-Callejas G, Piñeros-Avila M, Celis CA, Torrenegra R, Espinosa-Benitez A, Pestana-Nobles R, Yosa-Reyes J. 2024. Natural 2′,4-dihydroxy-4′,6′-dimethoxy chalcone isolated from *Chromolaena tacotana* inhibits breast cancer cell growth through autophagy and mitochondrial apoptosis. Plants 13 (5): 570. DOI: 10.3390/plants13050570.

Minarti, Cahyana AH, Darmawan A. 2021. Isolation, characterization and antidiabetic activity of phenolic compounds isolated from *Macaranga magna* Turrill. Rasayan J Chem 14 (4): 2420-2427. DOI: 10.31788/RJC.2021.1446290.

Naguib MM, Valvano MA. 2018. Vitamin E increases antimicrobial sensitivity by inhibiting bacterial lipocalin antibiotic binding. mSphere 3 (6): e00564-18. DOI: 10.1128/mSphere.00564-18.

Nyalo PO, Omwenga GI, Ngugi MP. 2023. Antibacterial properties and GC-MS analysis of ethyl acetate extracts of *Xerophyta spekei* (Baker) and *Grewia tembensis* (Fresen). Heliyon 9 (3): e14461. DOI: 10.1016/j.heliyon.2023.e14461.

Pires DEV, Blundell TL, Ascher DB. 2015. pkCSM: Predicting small-molecule pharmacokinetic and toxicity properties using graph-based signatures. J Med Chem 58 (9): 4066-4072. DOI: 10.1021/acs.jmedchem.5b00104.

Preethi, Hegde K. 2025. Traditional applications, phytochemical profiling and advanced pharmacological properties of plant *Macaranga peltata*. Intl J Pharm Sci 3 (3): 2683-2689. DOI: 10.5281/zenodo.15093397.

Priya D, Hani U, Haider N, Talath S, Shanmugarajan D, Prabitha P, Archana P, Kumar BRP. 2024. Novel PPAR-γ agonists as potential neuroprotective agents against Alzheimer's disease: Rational design, synthesis, in silico evaluation, PPAR-γ binding assay and transactivation and expression studies. RSC Adv 14: 33247-33266. DOI: 10.1039/d4ra06330a.

Rasoulpoor S, Shohaimi S, Salari N, Vaisi-Raygani A, Rasoulpoor S, Shabani S, Jalali R, Mohammadi M. 2021. *Candida albicans* skin infection in patients with type 2 diabetes: A systematic review and meta-analysis. J Diabetes Metab Disord 20 (1): 665-672. DOI: 10.1007/s40200-021-00797-0.

Razafindrakoto ZR, Tombozara N, Ramanitrahasimbola D, Andrianjara C, Zhao M, Marchioni E, Rakotondramanana DA, David JD. 2024. In silico ADMET and anti-inflammatory profiles of stigmast-4-e*n*-3-one and isolation of isovanillin as the antioxidant principle of *Imperata cylindrica* (L.) P. Beauv. Nat Prod Res 39 (10): 2679-2686. DOI: 10.1080/14786419.2024.2305649.

Redfern WS, Carlsson L, Davis AS, Lynch WG, MacKenzie I, Palethorpe S, Siegl PKS, Strang I, Sullivan AT, Wallis R, Camm AJ, Hammond TG. 2003. Relationships between preclinical cardiac electrophysiology, clinical QT interval prolongation and torsade de pointes for a broad range of drugs: Evidence for a provisional safety margin in drug development. Cardiovasc Res 58 (1): 32-45. DOI: 10.1016/S0008-6363(02)00846-5.

Rodríguez B, Pacheco L, Bernal I, Piña M. 2023. Mechanisms of action of flavonoids: Antioxidant, antibacterial and antifungal properties. Cienc Ambient Clima 6 (2): 33-66. DOI: 10.22206/cac.2023.v6i2.3021.

Rosamah E, Haqiqi MT, Putri AS et al. 2023. The potential of *Macaranga* plants as skincare cosmetic ingredients: A review. J Appl Pharm Sci 13: 1-12. DOI: 10.7324/japs.2023.77745.

Roy A, Khan A, Ahmad I, Alghamdi S, Rajab BS, Babalghith AO, Alshahrani MY, Islam S, Islam MR. 2022. Flavonoids: A bioactive compound from medicinal plants and its therapeutic applications. BioMed Res Intl 2022: 5445291. DOI: 10.1155/2022/5445291.

Sahidin I, Wahyuni, Malaka MH, Fristiohady A, Saleh A, Marianti A. 2019. Antibacterial and radical scavenger activities of extract and compounds of wualae (*Etlingera elatior*) stems from Southeast Sulawesi. IOP Conf Ser: Mater Sci Eng 546: 062027. DOI: 10.1088/1757-899X/546/6/062027.

Salleh WMNHW, Razak N, Farediah A. 2017. Phytochemicals and biological activities of *Macaranga hosei* and *Macaranga constricta* (Euphorbiaceae). Marmara Pharm J 21: 881-888. DOI: 10.12991/mpj.2017.11.

Sangboonruang S, Semakul N, Obeid MA, Ruano M, Kitidee K, Anukool U, Pringproa K, Chantawannakul P, Ferro VA, Tragoolpua Y, Tragoolpua K. 2021. Potentiality of melitt*in*-loaded niosomal vesicles against vancomyci*n*-intermediate *Staphylococcus aureus* and staphylococcal skin infection. Intl J Nanomedicine 16: 7639-7661. DOI: 10.2147/ijn.s325901.

Sharma A, Biharee A, Kumar A, Jaitak V. 2020. Antimicrobial terpenoids as a potential substitute in overcoming antimicrobial resistance. Curr Drug Targets 21 (14): 1476-1494. DOI: 10.2174/1389450121666200520103427.

Soccio RE, Chen ER, Lazar MA. 2014. Thiazolidinediones and the promise of insulin sensitization in type 2 diabetes. Cell Metab 20 (4): 573-591. DOI: 10.1016/j.cmet.2014.08.005.

Talapko J, Juzbašić M, Matijević T, Pustijanac E, Bekić S, Kotris I, Škrlec I. 2021. *Candida albicans*-The virulence factors and clinical manifestations of infection. J Fungi 7: 79. DOI: 10.3390/jof7020079.

Thawabteh AM, Ghanem AW, AbuMadi S, Thaher D, Jaghama W, Karaman R, Scrano L, Bufo SA. 2024. Antibacterial activity and antifungal activity of monomeric alkaloids. Toxins 16 (11): 489. DOI: 10.3390/toxins16110489.

Trott O, Olson AJ. 2010. AutoDock Vina: Improving the speed and accuracy of docking with a new scoring function, efficient optimization, and multithreading. J Comput Chem 31: 455-461. DOI: 10.1002/jcc.21334.

Tsunoda T, Samadi A, Burade S, Mahmud T. 2022. Complete biosynthetic pathway to the antidiabetic drug acarbose. Nat Commun 13 (1): 3455. DOI: 10.1038/s41467-022-31232-4.

Ullah A, Munir S, Badshah SL, Khan N, Ghani L, Poulson BG, Emwas A-H, Jaremko M. 2020. Important flavonoids and their role as a therapeutic agent. Molecules 25 (22): 5243. DOI: 10.3390/molecules25225243.

Vaou N, Stavropoulou E, Voidarou C, Tsigalou C, Bezirtzoglou E. 2021. Towards advances in medicinal plant antimicrobial activity: A review study on challenges and future perspectives. Microorganisms 9 (10): 2041. DOI: 10.3390/microorganisms9102041.

Vishwakarma M, Haider T, Soni V. 2024. Update on fungal lipid biosynthesis inhibitors as antifungal agents. Microbiol Res 278: 127517. DOI: 10.1016/j.micres.2023.127517.

Wijaya IKWA, Masfufatun M. 2022. Potensi lidah buaya (*Aloe vera*) sebagai antimikroba dalam menghambat pertumbuhan beberapa fungi: Literature review. J Kedokteran dan Kesehatan 18 (2): 202-211. DOI: 10.24853/jkk.18.2.202-211. [Indonesian]

Wood SJ, Kuzel TM, Shafikhani SH. 2023. *Pseudomonas aeruginosa*: Infections, animal modeling, and therapeutics. Cells 12 (1): 199. DOI: 10.3390/cells12010199.

Yan Y, Li X, Zhang C, Lv L, Gao B, Li M. 2021. Research progress on antibacterial activities and mechanisms of natural alkaloids: A review. Antibiotics 10 (3): 318. DOI: 10.3390/antibiotics10030318.

Zeleke ZZ. 2022. Flavonoid and stilbene cytotoxic phytochemicals isolated from genus *Macaranga* for the treatment of cancer cells: A review. J Commun Med 5 (2): 1045.

Zhou Y, Zhou Z, Zheng L, Gong Z, Li Y, Jin Y, Huang Y, Chi M. 2023. Urinary tract infections caused by uropathogenic *Escherichia coli*: Mechanisms of infection and treatment options. Intl J Mol Sci 24 (13): 10537. DOI: 10.3390/ijms241310537.

Zore GB, Thakre AD, Jadhav S, Karuppayil SM. 2011. Terpenoids inhibit *Candida albicans* growth by affecting membrane integrity and arrest of cell cycle. Phytomedicine 18 (13): 1181-1190. DOI: 10.1016/j.phymed.2011.03.008.

Zouine N, El Ghachtouli N, El Abed S, Koraichi SI. 2024. A comprehensive review on medicinal plant extracts as antibacterial agents: Factors, mechanism insights and future prospects. Sci Afr 26: e02395. DOI: 10.1016/j.sciaf.2024.e02395.